Article

Current European flood-rich period exceptional compared with past 500 years

https://doi.org/10.1038/s41586-020-2478-3

Received: 25 November 2019

Accepted: 21 May 2020

Published online: 22 July 2020

Check for updates

Günter Blöschl[1,35] ✉, Andrea Kiss[1,35], Alberto Viglione[2,35], Mariano Barriendos[3], Oliver Böhm[4], Rudolf Brázdil[5,6], Denis Coeur[7], Gaston Demarée[8], Maria Carmen Llasat[9], Neil Macdonald[10], Dag Retsö[11], Lars Roald[12], Petra Schmocker-Fackel[13], Inês Amorim[14], Monika Bělínová[6], Gerardo Benito[15], Chiara Bertolin[16], Dario Camuffo[17], Daniel Cornel[18], Radosław Doktor[19], Líbor Elleder[20], Silvia Enzi[21], João Carlos Garcia[22], Rüdiger Glaser[23], Julia Hall[1], Klaus Haslinger[2], Michael Hofstätter[24], Jürgen Komma[1], Danuta Limanówka[25], David Lun[1], Andrei Panin[26,27], Juraj Parajka[1], Hrvoje Petrić[28], Fernando S. Rodrigo[29], Christian Rohr[30], Johannes Schönbein[23], Lothar Schulte[31], Luís Pedro Silva[32], Willem H. J. Toonen[33], Peter Valent[1,34], Jürgen Waser[18] & Oliver Wetter[30]

There are concerns that recent climate change is altering the frequency and magnitude of river floods in an unprecedented way[1]. Historical studies have identified flood-rich periods in the past half millennium in various regions of Europe[2]. However, because of the low temporal resolution of existing datasets and the relatively low number of series, it has remained unclear whether Europe is currently in a flood-rich period from a long-term perspective. Here we analyse how recent decades compare with the flood history of Europe, using a new database composed of more than 100 high-resolution (sub-annual) historical flood series based on documentary evidence covering all major regions of Europe. We show that the past three decades were among the most flood-rich periods in Europe in the past 500 years, and that this period differs from other flood-rich periods in terms of its extent, air temperatures and flood seasonality. We identified nine flood-rich periods and associated regions. Among the periods richest in floods are 1560–1580 (western and central Europe), 1760–1800 (most of Europe), 1840–1870 (western and southern Europe) and 1990–2016 (western and central Europe). In most parts of Europe, previous flood-rich periods occurred during cooler-than-usual phases, but the current flood-rich period has been much warmer. Flood seasonality is also more pronounced in the recent period. For example, during previous flood and interflood periods, 41 per cent and 42 per cent of central European floods occurred in summer, respectively, compared with 55 per cent of floods in the recent period. The exceptional nature of the present-day flood-rich period calls for process-based tools for flood-risk assessment that capture the physical mechanisms involved, and management strategies that can incorporate the recent changes in risk.

Historical flood context

In recent decades, numerous devastating floods have occurred in Europe, with enormous economic damage[3]. Flood data over the past 50 years suggest that some parts of Europe are experiencing upward flood trends[4], but it has been unclear whether we are currently in a flood-rich period (more frequent and bigger floods than usual in extent and/or magnitude) and, if so, how unusual it is relative to other flood-rich periods during the past 500 years. An exceptional flood-rich period in recent decades would require more intensive and perhaps different adaption measures than a less unusual period. To understand whether recent decades are indeed exceptional, one needs to identify flood-rich periods and their characteristics in past centuries and compare them with recent decades.

The existence of flood-rich periods in the past 500 years has been demonstrated for several individual catchments in Europe based on historical documentary evidence[5–8] and mountain lake sediments[9]. One of the few available regional studies (19 documentary-based data series) identified 1540–1600, 1640–1700, 1730–1790 and 1790–1840 as flood-rich periods in central Europe[2], which is roughly consistent with sedimentary evidence from a set of Alpine lakes[10] and six floodplains[11] in central Europe. Several authors have suggested that more frequent flooding in the Little Ice Age (1300–1870), and specifically the Late Maunder Solar Minimum (1675–1725), can be related to lower air temperatures[2,6,8,12], but a more universal relationship with air temperatures for other flood-rich periods has not been identified[7,11,13]. Temperature anomalies can be considered a proxy for changes in the atmospheric

A list of affiliations appears at the end of the paper.

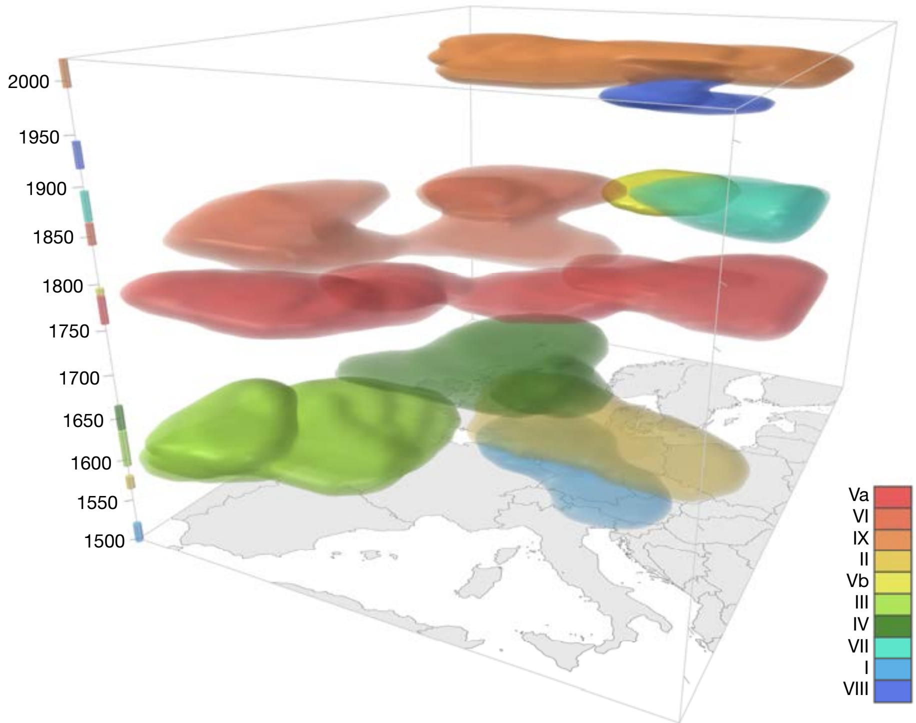

Fig. 1 | Flood-rich periods in Europe in the past 500 years. Periods are coloured by their rank, with red (period Va) indicating the strongest and blue (period VIII) indicating the weakest period (Table 1). For a dynamic visualization, see Supplementary Video 1.

circulation system and are therefore of relevance for assessing past and future changes in flood frequency.

Here we analyse the most comprehensive dataset of 103 sub-annual flood series over the past 500 years, covering all regions of Europe (Extended Data Fig. 1), to examine the existence and characteristics of flood-rich periods.

Reconstructing historical flood frequency

The flood series are based on the collation of published and unpublished series based on chronicles, annals, administrative and legal records, newspapers, and private and official correspondence (Extended Data Table 1). We almost exclusively used contemporary documentation (that is, written shortly after the flood events) because of its higher reliability relative to non-contemporary documentation. The documentation included direct indicators, such as the level and spatial extent of flood waters relative to identifiable landmarks, and, to a lesser extent, indirect indicators such as their environmental or socio-economic impact. For each piece of evidence, a critical, historical source evaluation was conducted, using the local socio-economic and environmental history knowledge of the analysts, to minimize errors in dating, interpretation and other possible mistakes originating from social biases.

For 103 river reaches across Europe, the documentary evidence on individual floods was transformed into a three-scaled intensity index for the period 1500–2016. The total number of floods contained in the dataset is 9,576, of which 8,954 have a season assigned. To account for differences in the representativeness of different series in space, we assigned to each series a representativeness index, which reflects the level of confidence that important floods have been captured. To account for temporal observational biases, we assigned each year of each series a rank on a bias index that reflects the completeness of the source material in a historical context. Although there is inevitable subjectivity in assigning these indices, decisions are nonetheless made on the basis of expert judgement of the sources and phenomena in question.

The intensity indices of the series were spatially and temporally interpolated, accounting where possible for uncertainty and bias (see Methods), which resulted in a three dimensional matrix of flood intensities over Europe in the past 500 years with voxel size of 41 km × 48 km × 4 years. This matrix was used to identify contiguous flood-rich periods in space and time by applying an algorithm that connects neighbouring voxels that exceed an intensity threshold. We ranked these flood-rich periods by the sum of the scaled space–time extent and the scaled mean flood intensity. Based on a 500-year central European air temperature reconstruction[14], which we consider to currently be the highest-quality multi-centennial reconstruction in Europe and to be spatially representative (see Methods), we compared the average air temperatures of these flood-rich periods with those of the interflood periods before and after. Additionally, we analysed the seasonality of flood occurrence in the flood-rich and interflood periods.

Flood-rich periods in the past 500 years

Here we find that the past three decades were among the most flood-rich in Europe during the past 500 years, and that this period differs from other flood-rich periods in terms of its extent, associated air temperatures and flood seasonality.

The nine flood-rich periods identified are rather regularly distributed in time, but the latest 30-year period is separated from past periods by a 90-year disaster gap in most of Europe with the occurrence of few floods (Fig. 1, 2; Table 1), in line with historical flood impact research[15]. The most highly ranked flood-rich periods, on the basis of their space–time extent and flood intensity, were 1560–1580 (period II, in western and central Europe), 1760–1800 (period V, in most of Europe), 1840–1870 (period VI, in western and southern Europe) and 1990–2016 (period IX, in western and central Europe) (Table 1, Supplementary Video 1).

Individually, the nine flood-rich periods cover only part of Europe, with areas between 0.41×10^6 km^2 and 1.83×10^6 km^2 (Extended Data Table 2), out of a total land area of 3.9×10^6 km^2 examined. There is a

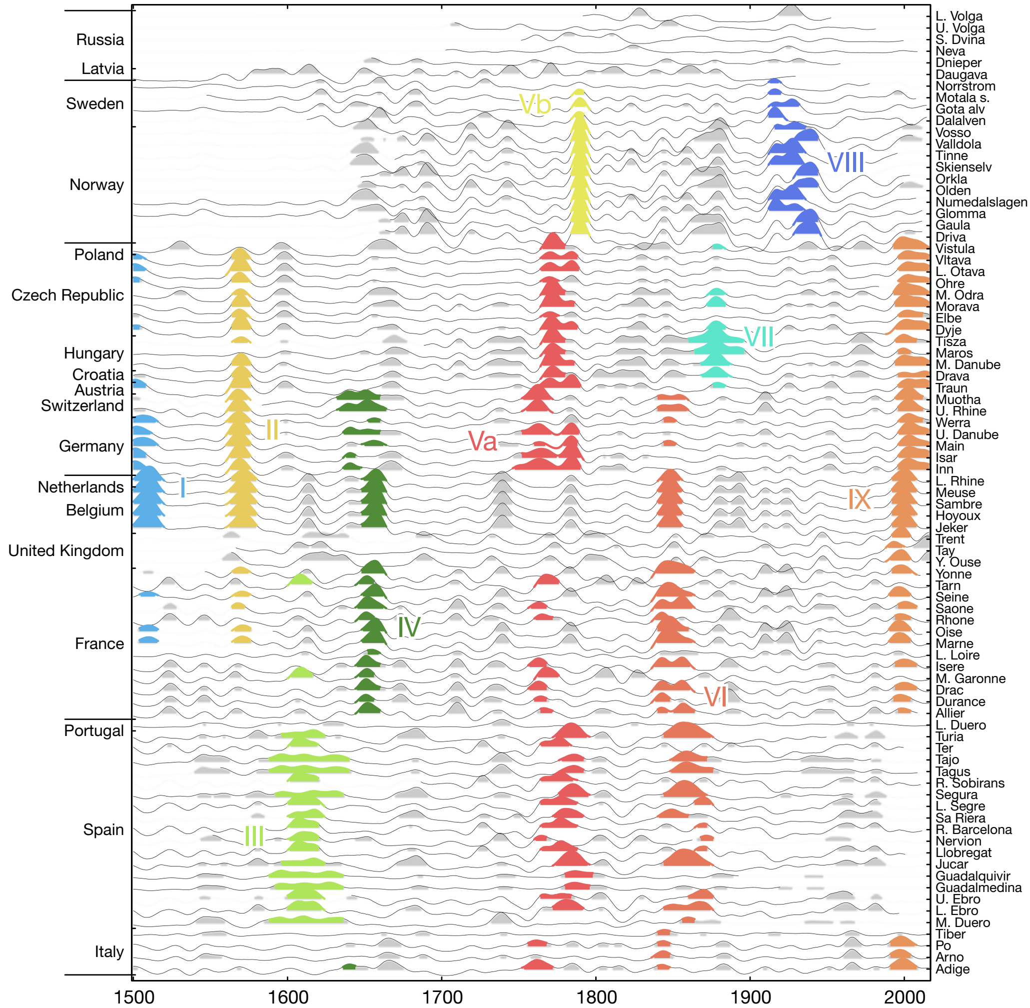

Fig. 2 | Flood intensities and flood-rich periods. Flood intensities have been interpolated in space and time (thin black lines), and the flood-rich periods identified are shown as coloured areas. For numbers of flood-rich periods see Table 1 and Extended Data Table 2. Abbreviations are defined in Extended Data Table 1. Grey areas indicate years that exceed the flood intensity threshold and are not in one of the identified flood-rich periods. Countries (left vertical axis) are grouped by region (from top to bottom: eastern, northern, central, western and southern Europe).

tendency for flood-rich periods to occur more often in central and western Europe than in other regions (Figs. 1 and 3).

The most recent flood-rich period is 1990–2016, the second largest in spatial extent (1.77×10^6 km^2) and the third largest in spatio-temporal extent (18.7×10^6 km^2 yr), indicating that it not only covered a large part of Europe, but also had a considerable duration in time (Extended Data Table 2). 2016 is the end of the data but possibly not the end of this flood-rich period.

The average air temperatures in most central European flood-rich periods were around 0.3 °C lower than those in the intervals between flood-rich periods, termed interflood periods (Fig. 4). Flood-rich period II was particularly cold and is known for the great glacier advances in the Alps[16]. The confidence bounds of temperatures in most flood-rich periods of the past versus the interflood periods in Fig. 4b are below the 1:1 line, indicating that the differences are statistically significant. The only exception was period IV (1630–1660), with average annual temperature similar to those of the interflood periods, resulting from warm summers; however, autumns and winters when most of the floods occurred were notably colder than usual[17]. This is consistent with the other flood-rich periods that were colder overall than interflood periods. In other parts of Europe, there is also a tendency for flood-rich periods I to VIII to be colder than the interflood periods, with differences of about 0.3 °C and 0.2 °C in western and southern Europe, respectively (Extended Data Fig. 4). In contrast, the most recent flood-rich period IX was on average about 1.4 °C warmer than the previous interflood period in all regions (Fig. 4b).

The time of year when floods most often occur differs between regions and between periods (Fig. 5, Extended Data Table 1). In central Europe, floods mainly occur in summer. In the central European flood-rich and interflood periods of the past, 41% and 42% of the floods occurred in summer, respectively. In contrast, during the recent flood period IX, 55% of the floods occurred in summer. The confidence bounds for the summer flood frequencies (right and middle red bars) in Fig. 5b do not overlap, indicating that the differences between the recent flood period IX and previous periods are significant rather than occurring by chance. In southern Europe, the corresponding frequencies for floods in autumn, which is the dominant flood season, increased from 43% (flood-rich) and 41% (interflood) to 54% (flood period IX) (Extended Data Fig. 5). In western Europe, the corresponding frequencies for floods in winter (the dominant flood season) increased from 49% (flood-rich) and 46% (interflood) to 55% (flood period IX) (Extended Data Fig. 5).

Flood processes and implications

Although there is some overlap between flood-rich periods detected here and those found previously in central Europe based on 19 series[2] (their periods, 1540–1600, 1640–1700 and 1730–1790, approximately

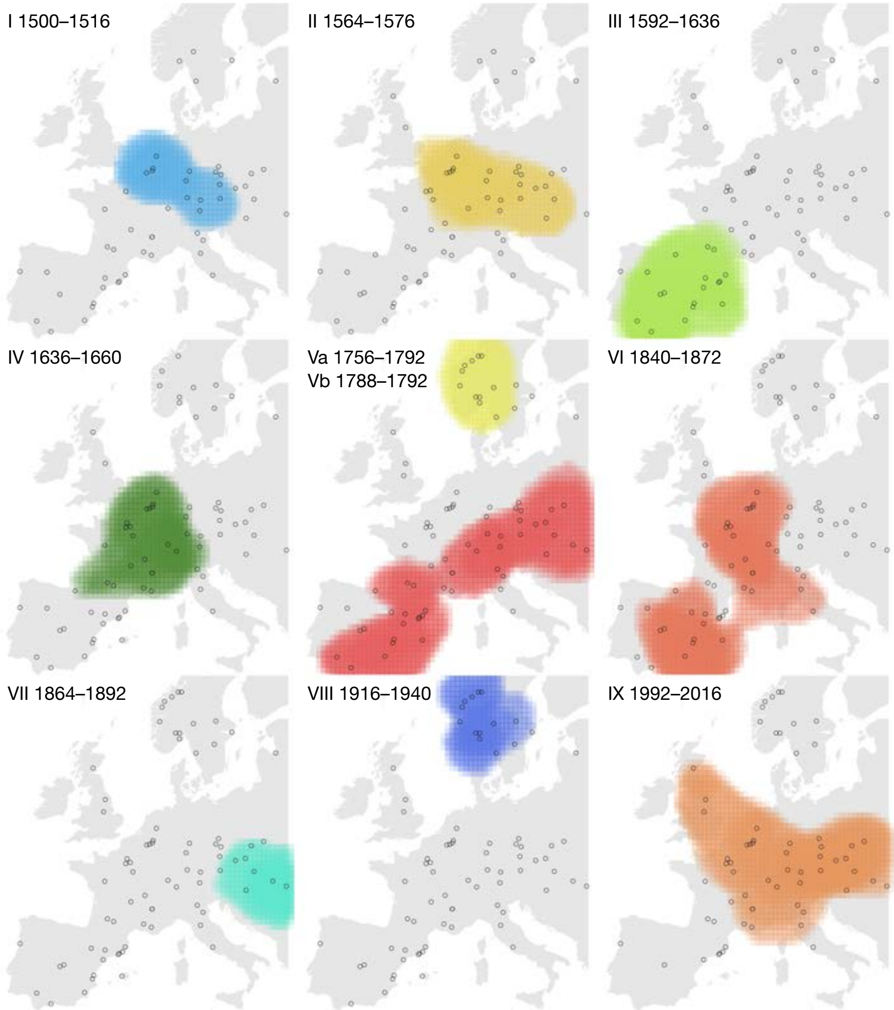

Fig. 3 | Flood-rich periods in Europe. For numbers, see Table 1 and Extended Data Table 2. Periods are coloured by their rank, with red (period Va) indicating the strongest and blue (period VIII) indicating the weakest period. Also see Extended Data Table 2 for the rank.

match periods II, IV and V here), their last period, 1790–1840, does not emerge as a flood-rich period here. Similarly, the Late Maunder period of low solar intensity (1675–1725) sometimes associated with flood occurrence in Europe[6] was not particularly flood-rich on a European level. The extent of the recent flood-rich period IX is consistent with the increasing trends in flood discharges observed in northwestern and central Europe in recent decades[4].

Previous analyses did not find coherent flood–temperature relationships at a European scale[6–8], which may partly reflect the low number of high-resolution series. At a local to regional scale (for example, Bohemia, eastern Spain) and in some periods (for example, Late Maunder solar minimum and eighteenth to nineteenth century), flood–temperature associations were demonstrated[6,18]. Our new comprehensive flood dataset provides clear evidence that such a relationship exists across Europe over the past 500 years.

The most important flood-rich period in our ranking, period V (1760–1800), occurred during the decades preceding the French revolution. Notably lower temperatures also prevailed during this period. Air-pressure reconstructions[19] suggest that there was frequent polar air intrusion into North America, the North Atlantic region and western Europe associated with an expanded polar cell, and lower north–south air-pressure gradients (negative North Atlantic Oscillation (NAO) index), pointing towards frequent atmospheric blocking situations in Europe[20,21]. In the 1780s, the sea ice extent around Iceland was at its greatest during the past 500 years[22]. The 1783 Lakigigar volcanic eruption in Iceland may have further contributed to lowering the temperatures[23].

Temperature is the most easily observed and most predictable parameter of a changing climate system. Although flood-producing precipitation is not necessarily driven by air-temperature anomalies, both are controlled by large-scale atmospheric circulations and ocean

Table 1 | Flood-rich periods in Europe since 1500

Period	Full time period	Spatial extent (regions)	Rank
I	1500–1520	Western Europe, central Europe	9
II	1560–1580	Western Europe, central Europe	4
III	1590–1640	Iberia, southern France	6
IV	1630–1660	Western Europe, west-central Europe, northern Italy	7
V	1750–1800	Va: central Europe, western Europe, southern Europe	1
		Vb: Scandinavia	5
VI	1840–1880	Western Europe, southern Europe	2
VII	1860–1900	East-central Europe	8
VIII	1910–1940	Scandinavia	10
IX	1990–2016*	Western Europe, central Europe, Italy	3

Regions are defined in Methods. Rank 1 (period Va) indicates the strongest and rank 10 indicates the weakest period (see Extended Data Fig. 2). Va and Vb were given a combined name because of their overlap in time.
*2016 is the end of the data but possibly not the end of period IX.

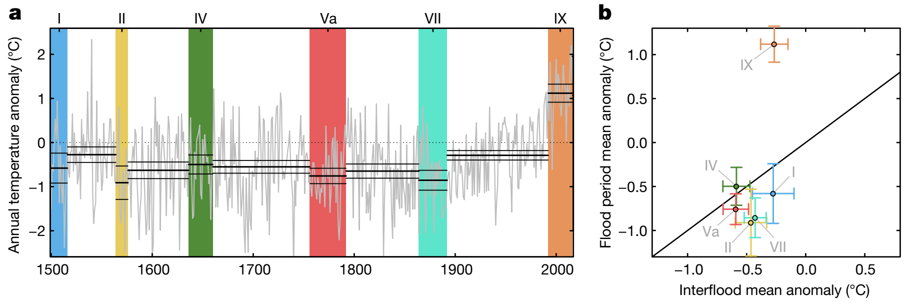

Fig. 4 | Anomalies of annual air temperatures from their 1961–1990 mean within and outside flood-rich periods in central Europe. a, Time series of air temperature anomalies (grey line) and their averages and 90% confidence bounds (black lines), and flood-rich periods indicated by coloured bars. **b**, Relationship between average temperature anomalies in flood-rich periods and those of the intervals in between. Error bars show 90% confidence bounds. Colours correspond to those of the flood-rich periods in **a**. Only the flood-rich periods that affected central Europe are shown here. For other regions, see Extended Data Fig. 4.

interactions[24]. In summer, the relationship between temperature and precipitation tends to be negative, as precipitation associated with cyclones implies more cloud cover and less solar radiation[25]. In winter, in contrast, there is a tendency for cyclones to transport moist and relatively warm air masses from the Atlantic to Europe, resulting in a positive relationship[26]. Spatio-temporal variations of precipitation and flooding depend on the NAO because of the link between NAO and the position of Atlantic storm tracks[24,27,28]. In winter, enhanced cyclone activity occurs in northern Europe during positive NAO phases, whereas in southern Europe this is the case during negative NAO phases[29], as the positions of Atlantic storm tracks migrate northward or southward, respectively. The decadal oscillations of the storm track position also lead to subcontinental temperature variations through the redistribution of cloud cover and precipitation as a result of internal climate variability[25,30]. The exact mix of atmospheric influences driving past flood-rich periods remains an open question that will require further work. We used a central European air temperature reconstruction here, and future work should incorporate further regionally specific reconstructions once available for the past 500 years.

Another factor contributing to higher floods in cold periods is soil moisture. Lower temperatures lead to less evaporation and hence higher soil moisture, which in turn results in larger floods, for the same rainfall[31,32]. The June 2013 flood in central Europe is an example of this. The preceding winter and spring were cold, soil moisture was much higher than usual and thus the flood was much larger than floods with dry antecedent soils[33]. Although the temperature–precipitation relationship in Europe depends on the season, annual rather than seasonal temperatures are analysed here so that not only flood event properties but also antecedent soil moisture and snow conditions are considered, which can be relevant for flood magnitudes over multiple-seasons.

During the past 30 years, hydroclimatic conditions over Europe have shifted to their millennial boundaries with a dry anomaly in southern Europe and a wet anomaly in central and northern Europe[34]. These changes appear to be caused by a persistent anomalous circulation regime of frequent low-pressure systems over the east Atlantic and western Europe[34]. Observational data suggest this pattern to be associated with a warm sea-surface-temperature anomaly in the Northern Atlantic Ocean[34,35], positive Atlantic multidecadal oscillation (AMO) and negative NAO, resulting in conditions that are likely to cause heavy precipitation through intense cyclone development and frequent blocking over western and central Europe[36–38]. Although contemporary air temperatures are much higher, there are similarities to the atmospheric circulation regime that prevailed in period V (1760–1800). However, climate model simulations suggest that present and future precipitation increases in Europe may be driven more by thermodynamics, that is, the higher water-holding capacity of a warmer atmosphere, than by changes in circulation[30,39], with increased evaporation and shallower snow packs also modulating floods[4]. It is therefore not clear how long the current flood-rich period IX will continue.

Systematic records have demonstrated that the timing of river floods in Europe has changed since 1960[40]. Figure 5 and Extended Data Fig. 5 demonstrate, however, that a change towards more frequent summer floods in central Europe, more frequent winter floods in western Europe and more frequent autumn floods in southern Europe started earlier than this, around 1940. The finding of increasing flood occurrence in the dominant flood season in all regions of Europe since 1960 in this paper is consistent with trends in flood timing and associated flood-generating processes, such as earlier snowmelt and fewer ice-jam floods in central Europe, and a seasonal shift of winter storms in the Atlantic region of Europe[2,4,40–42]. In the Mediterranean, enhanced evaporation and convective activity have increased the frequency of autumn floods[4,43,44].

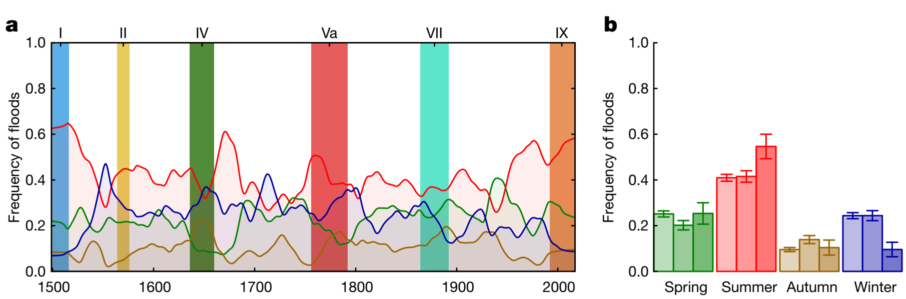

Fig. 5 | Seasonality of floods within and outside flood-rich periods in central Europe. a, Time series of smoothed frequency of floods in four seasons (green line, spring; red, summer; brown, autumn; blue, winter) and flood-rich periods indicated by coloured bars. **b**, Frequency of floods in four seasons. Left bars, interflood periods; middle bars, flood-rich periods of the past; right bars, flood-rich period IX (1990–2016). Error bars show 90% confidence bounds.

The European analysis presented here is a globally unique large-scale, high-resolution identification of flood-rich periods over multiple centuries. In other continents, flood-rich periods have been identified more locally. For example, in the states of Tabasco and Chiapas, Mexico, floods clustered during 1650–1680 and 1920–1950[45], which indicates some overlap with northern Europe (Fig. 2). At the River Paraná in South America the 1590s, 1620s, 1740s and 1770s were flood-rich[46], but they were mainly due to El Niño events, so one would expect different causal mechanisms from Europe. In Asia, millennial-scale investigations suggest that larger floods occurred between 1500 and 1700 on the River Yangtze[47].

Our research advances the global study of flood sensitivity to climate variability. Eventually, it may be possible to draw correlations between flood-rich periods across the globe that go beyond individual river basins and flood events. Flood management is currently strongly based on the analysis of systematic data in past decades. Extending the time window to past centuries would vastly strengthen the analysis, as they may provide a more complete guide to possible future flood changes, thereby allowing the creation of predictive tools that can enhance adaptation capacity at global and local scales. We have shown the strong potential of documentary data to contribute to such work.

The finding that the most recent 30 years are separated from past flood-rich periods by a 90-year disaster gap in most of Europe may explain why both the public and flood managers have been surprised by the severity of recent floods[48]. Flood-risk assessment tools and flood-risk management strategies need to account for the fact that we are currently in an exceptional flood-rich period in terms of timing of flood occurrence, magnitudes and spatial extent within Europe. Process-based models that capture the physical mechanisms in the atmosphere and rainfall–runoff transformation on the land surface, including the role of precipitation, soil moisture, snowmelt and seasonality in flood generation in both recent and historical times, will be an essential component of flood-risk assessment tools in a changing climate.

Online content

Any methods, additional references, Nature Research reporting summaries, source data, extended data, supplementary information, acknowledgements, peer review information; details of author contributions and competing interests; and statements of data and code availability are available at https://doi.org/10.1038/s41586-020-2478-3.

1. IPCC. *Special Report on Managing the Risks of Extreme Events and Disasters to Advance Climate Change Adaptation* (eds Field, C. B. et al.) (Cambridge Univ. Press, 2012).
2. Glaser, R. et al. The variability of European floods since AD 1500. *Clim. Change* **101**, 235–256 (2010).
3. UNDRR. *Global Assessment Report on Disaster Risk Reduction* (Geneva, 2019).
4. Blöschl, G. et al. Changing climate both increases and decreases European river floods. *Nature* **573**, 108–111 (2019).
5. Camuffo, D. & Enzi, S. in *Climatic Variations and Forcing Mechanisms of the Last 2000 Years* (eds Jones, P. et al.) 433–450 (Springer, 1996).
6. Brázdil, R. et al. Fluctuations of floods of the River Morava (Czech Republic) in the 1691–2009 period: interactions of natural and anthropogenic factors. *Hydrol. Sci. J*. **56**, 468–485 (2011).
7. Schmocker-Fackel, P. & Naef, F. Changes in flood frequencies in Switzerland since 1500. *Hydrol. Earth Syst. Sci*. **14**, 1581–1594 (2010).
8. Pichard, G., Arnaud-Fassetta, G., Moron, V. & Roucaute, E. Hydro-climatology of the Lower Rhône Valley: historical flood reconstruction (AD 1300–2000) based on documentary and instrumental sources. *Hydrol. Sci. J*. **62**, 1772–1795 (2017).
9. Wilhelm, B., Vogel, H., Crouzet, C., Etienne, D. & Anselmetti, F. S. Frequency and intensity of palaeofloods at the interface of Atlantic and Mediterranean climate domains. *Clim. Past* **12**, 299–316 (2016).
10. Wirth, S. B., Glur, L., Gilli, A. & Anselmetti, F. S. Holocene flood frequency across the Central Alps—solar forcing and evidence for variations in North Atlantic atmospheric circulation. *Quat. Sci. Rev*. **80**, 112–128 (2013).
11. Schulte, L. et al. Integration of multi-archive datasets for the development of a four-dimensional paleoflood model of alpine catchments. *Global Planet. Change* **180**, 66–88 (2019).
12. Retsö, D. Documentary evidence of historical floods and extreme rainfall events in Sweden 1400–1800. *Hydrol. Earth Syst. Sci*. **19**, 1307–1323 (2015).
13. Glur, L. et al. Frequent floods in the European Alps coincide with cooler periods of the past 2500 years. *Nat. Sci. Rep*. **3**, 2770 (2013).
14. Dobrovolný, P. et al. Monthly and seasonal temperature reconstructions for central Europe derived from documentary evidence and instrumental records since AD 1500. *Clim. Change* **101**, 69–107 (2010).
15. Pfister, C. The 'Disaster Gap' of the 20th century and the loss of traditional disaster memory. *Gaia* **18**, 239–246 (2009).
16. Nicolussi, K., Joerin, U. E., Kaiser, K. F., Patzelt, G. & Thurner, A. in *Global Change in Mountain Regions* (ed. Price, M. F.) 59–60 (Duncow Sapiens, 2006).
17. Glaser, R. *Klimageschichte Mitteleuropas: 1200 Jahre Wetter, Klima, Katastrophen* (Darmstadt Primus, 2013), 94.
18. Barriendos Vallve, M. & Martin-Vide, J. Secular climatic oscillations as indicated by catastrophic floods in the Spanish Mediterranean coastal area (14th–19th centuries). *Clim. Change* **38**, 473–491 (1998).
19. McNally, L. K. Reconstruction of late 18th century upper-air circulation using forensic synoptic analysis. *Hist. Meteorol*. **2**, 105–122 (2005).
20. Cornes, R. C., Jones, P. D., Briffa, K. R. & Osborn, T. J. Estimates of the North Atlantic Oscillation back to 1692 using a Paris–London westerly index. *Int. J. Climatol*. **33**, 228–248 (2013).
21. Slonosky, V. C., Jones, P. D. & Davies, T. D. Variability of the surface atmospheric circulation over Europe, 1774–1995. *Int. J. Climatol*. **20**, 1875–1897 (2000).
22. Ogilvie, A. E. J. in *Climate Since A.D. 1500* (eds Bradley, R. S. & Jones, P. D.) 92–117 (Routledge, 1992).
23. Brázdil, R. et al. European floods of the winter 1783/84: scenarios of an extreme event during the 'Little Ice Age'. *Theor. Appl. Climatol*. **100**, 163–189 (2010).
24. Woollings, T., Hannachi, A. & Hoskins, B. Variability of the North Atlantic eddy-driven jet stream. *Q. J. R. Meteorol. Soc*. **136**, 856–868 (2010).
25. Gagen, M. et al. North Atlantic summer storm tracks over Europe dominated by internal variability over the past millennium. *Nat. Geosci*. **9**, 630–635 (2016).
26. Hurrell, J. W. & Van Loon, H. in *Climatic Change at High Elevation Sites* (eds Diaz, H. F. et al.) 69–94 (Springer, 1997).
27. Nobre, G. G., Jongman, B., Aerts, J. C. J. H. & Ward, P. J. The role of climate variability in extreme floods in Europe. *Environ. Res. Lett*. **12**, 084012 (2017).
28. Steirou, E., Gerlitz, L., Apel, H., Sun, X. & Merz, B. Climate influences on flood probabilities across Europe. *Hydrol. Earth Syst. Sci*. **23**, 1305–1322 (2019).
29. Folland, C. K. et al. The summer North Atlantic Oscillation: past, present, and future. *J. Clim*. **22**, 1082–1103 (2009).
30. Raible, C., Messmer, M. B., Lehner, F., Stocker, T. & Blender, R. Extratropical cyclone statistics during the last millennium and the 21st century. *Clim. Past* **14**, 1499–1514 (2018).
31. Komma, J., Blöschl, G. & Reszler, C. Soil moisture updating by ensemble Kalman filtering in real-time flood forecasting. *J. Hydrol*. **357**, 228–242 (2008).
32. Grillakis, M. G. et al. Initial soil moisture effects on flash flood generation—a comparison between basins of contrasting hydro-climatic conditions. *J. Hydrol*. **541**, 206–217 (2016).
33. Blöschl, G., Nester, T., Komma, J., Parajka, J. & Perdigao, R. A. P. The June 2013 flood in the Upper Danube Basin, and comparisons with the 2002, 1954 and 1899 floods. *Hydrol. Earth Syst. Sci*. **17**, 5197–5212 (2013).
34. Markonis, Y., Hanel, M., Máca, P., Kyselý, J. & Cook, E. R. Persistent multi-scale fluctuations shift European hydroclimate to its millennial boundaries. *Nat. Commun*. **9**, 1767 (2018).
35. Sutton, R. T. & Dong, B. Atlantic Ocean influence on a shift in European climate in the 1990s. *Nat. Geosci*. **5**, 788–792 (2012).
36. Hofstätter, M. & Blöschl, G. Vb cyclones synchronized with the Arctic/North Atlantic Oscillation. *J. Geophys. Res. D* **124**, 3259–3278 (2019).
37. Hofstätter, M., Lexer, A., Homan, M. & Blöschl, G. Large-scale heavy precipitation over central Europe and the role of atmospheric cyclone track types. Int. *J. Clim* **38**, e497–e517 (2018).
38. Messmer, M., Gómez-Navarro, J. J. & Raible, C. C. Climatology of Vb cyclones, physical mechanisms and their impact on extreme precipitation over central Europe. *Earth Syst. Dynam*. **6**, 541–553 (2015).
39. Hawcroft, M., Walsh, E., Hodges, K. & Zappa, G. Significantly increased extreme precipitation expected in Europe and North America from extratropical cyclones. *Environ. Res. Lett*. **13**, 124006 (2018).
40. Blöschl, G. et al. Changing climate shifts timing of European floods. *Science* **357**, 588–590 (2017).
41. Berghuijs, W. R., Harrigan, S., Molnar, P., Slater, L. J. & Kirchner, J. W. The relative importance of different flood-generating mechanisms across Europe. *Wat. Resour. Res*. **55**, 4582–4593 (2019).
42. Xoplaki, E., Gonzalez-Rouco, J. F., Luterbacher, J. & Wanner, H. Wet season Mediterranean precipitation variability: influence of large-scale dynamics and trends. *Clim. Dyn*. **23**, 63–78 (2004).
43. Barrera-Escoda, A. & Llasat, M. C. Evolving flood patterns in a Mediterranean region (1301–2012) and climatic factors—the case of Catalonia. *Hydrol. Earth Syst. Sci*. **19**, 465–483 (2015).
44. Barriendos, M. & Rodrigo, F. S. Study of historical flood events on Spanish rivers, using documentary data. *Hydrol. Sci. J*. **51**, 765–783 (2006).
45. Valdés-Manzanilla, A. Historical floods in Tabasco and Chiapas during sixteenth–twentieth centuries. *Nat. Hazards* **80**, 1563–1577 (2016).
46. Prieto, M. R. ENSO signals in South America: rains and floods in the Paraná River region during colonial times. *Clim. Change* **83**, 39–54 (2007).
47. Tong, J., Quiang, Z., Deming, Z. & Yijin, W. Yangtze floods and droughts (China) and teleconnections with ENSO activities (1470–2003). *Quat. Int*. **144**, 29–37 (2006).
48. Merz, B., Vorogushyn, S., Lall, U., Viglione, A. & Blöschl, G. Charting unknown waters—on the role of surprise in flood risk assessment and management. *Wat. Resour. Res*. **51**, 6399–6416 (2015).

Publisher's note Springer Nature remains neutral with regard to jurisdictional claims in published maps and institutional affiliations.

[1]Institute of Hydraulic Engineering and Water Resources Management, Vienna University of Technology, Vienna, Austria. [2]Department of Environment, Land and Infrastructure Engineering (DIATI), Politecnico di Torino, Turin, Italy. [3]Department of History and Archaeology, University of Barcelona, Barcelona, Spain. [4]Institute of Geography, University of Augsburg, Augsburg, Germany. [5]Institute of Geography, Masaryk University, Brno, Czech Republic. [6]Global Change Research Institute, Czech Academy of Sciences, Brno, Czech Republic. [7]ACTHYS-Diffusion, Grenoble, France. [8]Royal Meteorological Institute of Belgium, Brussels, Belgium. [9]Department of Applied Physics, University of Barcelona, Barcelona, Spain. [10]Department of Geography and Planning, School of Environmental Sciences, University of Liverpool, Liverpool, UK. [11]Department of Economic History and International Relations, Stockholm University, Stockholm, Sweden. [12]Norwegian Water Resources and Energy Directorate, Oslo, Norway. [13]Hydrology Division, Federal Office for the Environment (FOEN), Bern, Switzerland. [14]Department of History, Political and International Studies, University of Porto, Porto, Portugal. [15]Department of Geology, National Museum of Natural Sciences, CSIC, Madrid, Spain. [16]Department of Mechanical and Industrial Engineering, Norwegian University of Science and Technology, Trondheim, Norway. [17]National Research Council, Institute of Atmospheric Sciences and Climate, Padua, Italy. [18]VRVis Research Center for Virtual Reality and Visualization, Vienna, Austria. [19]Centre for Flood and Drought Modelling, Institute of Meteorology and Water Management, National Research Institute, Warsaw, Poland. [20]Czech Hydrometeorological Institute, Prague, Czech Republic. [21]Kleio Studio Associate Research Company, Padua, Italy. [22]Faculty of Arts, University of Porto, Porto, Portugal. [23]Department of Physical Geography, University of Freiburg, Freiburg, Germany. [24]Climate Research Department, Central Institute of Meteorology and Geodynamics (ZAMG), Vienna, Austria. [25]Centre for Poland's Climate Monitoring, Institute of Meteorology and Water Management, National Research Institute, Cracow, Poland. [26]Institute of Geography, Russian Academy of Sciences, Moscow, Russia. [27]Lomonosov Moscow State University, Moscow, Russia. [28]Department of History, Faculty of Humanities and Social Sciences, University of Zagreb, Zagreb, Croatia. [29]Department of Chemistry and Physics, University of Almería, Almería, Spain. [30]Department of Economic, Social and Environmental History, Institute of History, University of Bern, Bern, Switzerland. [31]Department of Geography, University of Barcelona, Barcelona, Spain. [32]Transdisciplinary Research Centre Culture, Space and Memory, University of Porto, Porto, Portugal. [33]Department of Physical Geography, Utrecht University, Utrecht, The Netherlands. [34]Department of Land and Water Resources Management, Faculty of Civil Engineering, Slovak University of Technology in Bratislava, Bratislava, Slovakia. [35]These authors contributed equally: Günter Blöschl, Andrea Kiss, Alberto Viglione. ✉e-mail: bloeschl@hydro.tuwien.ac.at

Methods

Development of historical flood database

The development of the historical flood series from documentary evidence followed standard methods for flood magnitude classification. The evidence consisted of historical documentation including narratives (for example, chronicles), administrative sources, newspapers, and private and official correspondence (for example, letters). We used almost exclusively (over 90%) contemporary documentation, written shortly after the flood events, rather than non-contemporary documentation, because of its higher reliability[49]. The documentation always included direct indicators, such as the level and spatial extension of flood waters relative to identifiable landmarks and, in most cases, indirect indicators such as the environmental or socio-economic impact that provide complementary information. For each piece of evidence, a critical, historical source evaluation was conducted, using the local socio-economic and historical source knowledge of the analysts, to minimize errors in dating, interpretation and other possible mistakes originating from social biases.

Individual series do not necessarily originate from exactly the same location. Series 'HU01 Middle Danube' (see Extended Data Table 1), for example, was based on evidence from the Danube reach between Bratislava and Mohács, a reach of about 400 km, as this reach can be considered approximately homogeneous in terms of flood magnitude. Reaches were judged as approximately homogeneous if the sources at different locations along that reach usually suggested the same index value for the same event. In other cases, the information was more focused. For example, series 'ES19 Ter' is based on information from Girona only. Coordinates were assigned to each series representing the centre of gravity of the source information. For the series HU01 Middle Danube, for example, the coordinates were selected at Komárom, which is slightly upstream of the middle of the reach.

The documentary evidence was then transformed into a numerical intensity index. We applied the most widely used three-scaled index method, differentiating flood events into intensities i_f of notable (class 1), great (class 2) and extraordinary (class 3) magnitudes[50–52]. A flood was considered notable (class 1) if the flood waters exceeded the river banks, but not greatly; great (class 2) if they considerably exceeded the river banks, often over an extended period of time with local hydromorphological changes; and extraordinary (class 3) if the flood waters were much higher and spatially more extended than usual floods, often unexpected and with major disruption of daily life. Historical documents would typically refer to these three categories as flood, great flood and very great flood (or extraordinary flood or deluge), respectively[51]. Because the intensity index was mainly based on direct indicators, it is intended to reflect flood magnitudes, rather than flood damage. The index also accounted for the construction of flood protection measures such as levees[18]. For example, at Szeged in Hungary ('HU03 Tisza' series), a major levee system was constructed in the early 1880s. In the period before, a flood would be considered a notable (class 1) flood if the lower floodplain around the town, the pastures and some cultivated fields were inundated. In the period after, a flood would be considered a notable (class 1) flood if water greatly exceeded the quay (low-lying road along the shoreline) even though the pastures and the cultivated fields in the lower floodplain were not inundated because they were protected[51]. Similar differentiations were made for class 2 and class 3 floods. The effects of land-use change were assumed to be small, as 80% of the catchments were larger than 700 km^2, and land-use changes tend to be important only for small catchments[53]. This is because changes in the infiltration capacity of soils mainly affect flood generation resulting from thunderstorms in small catchments[53–55]. Additionally, for all series we identified (i) years known to have no floods, (ii) years with probably no floods, (iii) years that could either have no floods or simply have missing data (that is, no flood information) and (iv) years outside the period covered by the series.

To account for differences in the representativeness of different series in space, we assigned to each series a representativeness index u (1, low representativeness; 2, average representativeness; 3, high representativeness) that reflects the level of confidence that important floods have been captured, based on a holistic assessment of the completeness of the source material in a regional context. For example, the 'SE02 Motala strom' series was considered highly representative ($u = 3$) because there is high confidence that all the important floods have been captured, even though the total number of reported floods may be lower than in other stations. In this case, we have high confidence because of the nature of source type (consistent local chronicles and diaries)[12]. There is also a tendency for series of larger rivers to have higher representativeness than series of smaller rivers because of the higher population density and the more frequent presence of cities.

To account for temporal observational biases, we assigned to each year of each series a bias index, on a scale from 1 to 4, that reflects the completeness of the source material in a historical context. Index values from 1 to 4 indicate, respectively, no data; periods with possibly missing data; average; and periods with overly dense data compared with the average of that series. For example, 'AT01 Traun' for the period 1500–1600 benefited from the availability of weekly bridge master accounts, which make the data much more complete than later when such accounts were not available[56]. For most series, however, the more recent years are more complete.

A total of 103 river flood series were compiled. Out of these, 70 start in 1500; 82, 99 and 103 series start in or earlier than 1600, 1700 and 1800, respectively (Extended Data Figs. 1–3). The total number of floods contained in the dataset is 9,576, of which 8,954 have a season assigned. The seasons are spring (March–May), summer (June–August), autumn (September–November) and winter (December–February). There are 5,696 class 1 floods (notable), 2,616 class 2 floods (great) and 1,264 class 3 floods (extraordinary).

Interpolation

In interpolating flood intensity in space and time, only class 2 and 3 floods are used, since they are considered to be less affected by observation bias. This is because class 2 and 3 floods tend to result in higher disruption of the daily life than class 1 floods, which increases the societal relevance and thus the likelihood of being documented. When a series contained more than one event per year, the intensities of the individual events i_f were aggregated to one annual intensity i_a by $i_a = \sqrt{\sum i_f^2}$ where the summation is over the events of that year. To reduce some of the spatial correlations, only 83 out of the 103 series were used for interpolation, excluding series with similar intensities to neighbouring series either because they are nested catchments or derived from homogeneous flood regions (denoted 'supplementary' in Extended Data Fig. 1). Some spatial correlation may remain which may bias the results of the interpolation.

To reduce observation bias, zero intensities ($i_a = 0$) were added randomly in some of the years when no class 2 or 3 flood was recorded with probability $p_0(t) = 1 - (1 - p_f(t))^{\alpha}$, where the annual flood probability $p_f(t)$ was estimated from the occurrence of class 2 and 3 floods within a 100-year time window around the target year t. The exponent α was set to 10, based on test simulations. The consistency of the bias reduction method with the bias index (Extended Data Fig. 2) was checked visually by assessing how many zero values were added in periods characterized by different bias indices. In periods with possible missing data and in periods with overly dense data, the method added a smaller and larger number of zeroes than average, respectively, suggesting that the bias reduction method is consistent with the bias index. The validity of the bias reduction method was checked by examining whether monotonic trends appeared over the entire 500-year period in the interpolated flood intensities. Without bias correction, most major events would be identified in the second half of the 500-year period; but with bias correction, the events were more uniformly distributed in time and there were no monotonic trends in line with the historical expert assessment. The bias index was used to test the bias reduction method rather than to modify the flood intensity in each year and station individually, in order to enhance the repeatability and spatial consistency of the analysis.

The intensities i_a were interpolated using the thin plate spline regression algorithm of the *fastTps* function in the R package *fields*. The coordinates of the series were transformed into kilometres by an azimuthal equidistant projection centred at 51° N and 7° E. The interpolation is in space and time, so some equivalence of space and time is needed reflecting a typical relationship between the extent and duration of flood-rich periods in Europe. Based on space–time empirical variograms[57] of the intensities i_a and visual examination we chose a ratio of 50 km per year.

The *fastTps* function assigns a weight to each data point that reflects the inverse of its uncertainty. These weights were calculated based on the representativeness index u of each series and the annual flood intensity i_a, as $w = k(u/2)^2$ where k is 0.2, 1.0 and 1.5 for $i_a < 1.5$, $1.5 < i_a < 2.5$ and $i_a > 2.5$, respectively. The small weights of the 0 intensities were chosen to reflect their larger uncertainty. The possible drawback of this procedure is an element of subjectivity of the parameters, but the results were more plausible from a historical expert perspective, than when ignoring the differences in representativeness of the series. The smoothing and tapering range parameters of *fastTps* were set to 10 years and 20 years (or 1,000 km), respectively, based on an expert assessment of test simulations. A linear drift component was selected.

To increase the robustness of the procedure and assess the sensitivity of the results to adding 0 intensities, the space-time interpolation was repeated 50 times with 50 different realizations of 0 intensities. The resulting median i_i of the interpolated intensities represents a three-dimensional matrix of flood intensities i_i over Europe in the past 500 years with voxel size of about 41 km × 48 km × 4 yr. This matrix was used for identifying contiguous flood periods in space and time using an algorithm that connects neighbouring voxels that exceed an intensity threshold[58]. We set the threshold i_i^* to the 95% quantile of the interpolated i_i over the matrix ($i_i^* = 1.375$), which means that these contiguous periods collectively cover 5% of the space–time domain. A comparison of the flood-rich periods obtained for different realizations of 0 intensities showed some differences, but the main pattern remained. For example, the top ranked periods always remained at the top with similar spatial and temporal extents.

We calculated the core duration of the flood-rich periods as the time differences between the centres of voxels, and we calculated the areas and volumes as the number of voxels included times their individual area and volume, respectively. As the interest of this study was in the large flood-rich periods, we only kept periods with volumes larger than 78,711 km^2 yr (corresponding to 10 voxels) for further analysis. This resulted in a total of 74 flood-rich periods for which the projected area (km^2), the space-time extent or volume (km^2 yr), a scaled space-time extent (0 for the smallest of the 74 events, 1 for the largest), and the scaled mean intensity of the period were calculated. The periods were ranked by the sum of the scaled space–time extent and scaled mean intensity. The top periods thus identified were 1756–1792 followed by 1840–1872 and 1992–2016. Changing the ranking function slightly changed the ordering of the periods, but the largest periods always remained at the top. The top ten periods were given Roman numerals in chronological order (Extended Data Table 2). Two periods (Va and Vb) were given a combined name due to their overlap in time. The results are moderately sensitive to the ratio parameter. For example, changing it from 50 km yr to 100 km yr and 25 km yr changes the extent of period IX from 1.8 km^2 to 2.3 km^2 and 1.2×10^6 km^2, the duration from 25 years to 17 years and 25 years, and the volume from 19 to 23 and 14×10^6 km^2 yr, respectively. The positions in time and space of the centres of the periods change little in most cases, and the current top eight events remain in the list of top 10 events. The results show little sensitivity to the choice of the smoothing and tapering range parameters of the spline interpolation.

Air temperatures

We used a 500-year central European temperature reconstruction[14] to evaluate the air temperatures of the flood-rich periods, which we consider to currently be the highest quality reconstruction in Europe, as the annual correlations with other, more local, historical series in Europe are relatively high. The correlation coefficients with the series in Barcelona, central England and Stockholm are 0.67, 0.73 and 0.64, respectively[59–61] which indicates spatial representativeness over much of Europe. The data are temperature deviations (anomalies) from the mean 1961–1990 and have been derived from documentary sources such as chronicles, weather diaries, accounts, letters, newspapers and legal sources. Potential biases and limitations may derive from data coverage and calibration relationships varying in time. We chose annual rather than seasonal temperatures for the analysis because we intended to not only capture flood event properties, but also antecedent soil moisture and snow conditions which can be relevant for flood magnitudes over more than one season. Annual and seasonal temperature averages over decades are correlated with $r = 0.75$, 0.75 and 0.82 for summer, autumn and winter, respectively.

The average air temperatures of each flood-rich period were estimated separately for five regions in Europe: eastern Europe (Russia, Latvia), northern Europe (Sweden, Norway), central Europe (Poland, Czechia, Hungary, Austria, Switzerland, Germany), western Europe (the Netherlands, Belgium, Great Britain, France) and southern Europe (Portugal, Spain, Italy) (Extended Data Fig. 1). Based on the spatial locations of the flood-rich periods, eastern Europe showed some signal during period V (due to class 3 floods in 1760, 1761, 1770, 1771, 1777, 1779 and 1784, and eight class 2 floods) and period VII (due to a class 3 flood in 1877 and 13 class 2 floods), but this was too weak to be included (possibly a result of lower data density). In northern Europe, flood-rich periods Vb and VIII occurred, in central Europe I, II, IV, Va, VII, IX, in western Europe I, II, IV, Va, VI, IX, and in southern Europe III, Va, VI, IX. Additionally, average temperatures were estimated for periods between these flood-rich periods (termed interflood periods here). The 90% confidence bounds of these averages m_T were estimated by $m_T \pm 1.645\sqrt{\upsilon_T/n}$ where υ_T is the variance of the annual temperatures and n is the number of years in the period. Figure 4b and Extended Data Fig. 4b–d compare the average temperatures of the flood-rich periods with those of the interflood periods before and after (for period I only after, for period IX only before).

Seasonality analysis

The flood-rich periods were also analysed with respect to their average flood seasonality for the same five regions. In contrast to the interpolation of the intensities, for the seasonality all 103 series and all floods (including class 1 floods) were included in order to develop a more robust estimate of seasonality, which tends to vary considerably between events[62]. Including the floods classified as class 1 reduced uncertainty in the flood seasonality resulting from missing data. The analysis was performed considering all flood events — that is, in some cases more than one flood per year per site. As we were more interested in the seasonality of the large floods, while maintaining the robustness by including small events, we estimated the frequency of floods within each season as a weighted mean of the frequencies of each of the flood intensities, giving class 1, 2 and 3 floods weights of 1, 2 and 3, respectively.

The lines in Fig. 5a and Extended Data Fig. 5a–c show the frequency of floods in each season over the past 500 years applying a 30-year averaging window for central, southern and western Europe. In northern and eastern Europe, the number of floods was too low to make reliable inferences on changes in seasonal flood frequencies. Figure 5b and Extended Data Fig. 5b–d show the averages of the frequencies over all interflood periods, the past flood-rich periods (excluding the recent one), and the recent flood-rich period IX. The 90% confidence bounds of the averages p_s were estimated by $p_s \pm -1.645\sqrt{p_s(1-p_s)/n}$, where n is the number of years with floods whose season is known.

Data availability

The flood index data that were used in this paper and an extended list of references are available at https://github.com/tuwhydro/500yrfloods. The air temperature data are available at https://www.ncdc.noaa.gov/paleo-search/study/9970

Code availability

The data analysis was performed in R using the supporting package *fields* for the thin plate spline interpolation (function *fastTps*). The code used can be downloaded from https://github.com/tuwhydro/500yrfloods.

49. Brázdil, R. et al. in *Changes in Flood Risk in Europe* (ed. Kundzewicz, Z. W.) 121–166 (CRC, 2012).
50. Sturm, K. et al. Floods in central Europe since AD 1500 and their relation to the atmospheric circulation. *Petermanns Geogr. Mitt*. **145**, 14–23 (2001).
51. Salinas, J.L., Kiss, A., Viglione, Viertl, R. & Blöschl. G. A fuzzy Bayesian approach to flood frequency estimation with imprecise historical information. *Wat. Resour. Res*. **52**, 6730–6750 (2016).
52. Kiss, A. *Floods and Long-Term Water-Level Changes in Medieval Hungary*, 280–285 (Springer, 2019).
53. Viglione, A. et al. Attribution of regional flood changes based on scaling fingerprints. *Wat. Resour. Res*. **52**, 5322–5340 (2016).
54. Hall, J. et al. Understanding flood regime changes in Europe: a state of the art assessment. *Hydrol. Earth Syst. Sci*. **18**, 2735–2772 (2014).
55. Rogger, M. et al. Land-use change impacts on floods at the catchment scale—challenges and opportunities for future research. *Wat. Resour. Res*. **53**, 5209–5219 (2017).
56. Rohr, C. *Extreme Naturereignisse im Ostalpenraum. Naturerfahrung im Spätmittelalter und am Beginn der Neuzeit*, 558–562 (Köln Böhlau, 2007).
57. Skøien, J. & Blöschl, G. Catchments as space-time filters—a joint spatio-temporal geostatistical analysis of runoff and precipitation. *Hydrol. Earth Syst. Sci*. **10**, 645–662 (2006).
58. Haslinger, K. & Blöschl, G. Space-time patterns of meteorological drought events in the European Greater Alpine Region over the past 210 years. *Wat. Resour. Res*. **53**, 9807–9823 (2017).
59. Prohom, M., Barriendos, M. & Sanchez-Lorenzo, A. Reconstruction and homogenization of the longest instrumental precipitation series in the Iberian Peninsula (Barcelona, 1786–2014). *Int. J. Climatol*. **36**, 3072–3087 (2016).
60. Parker, D. E. & Horton, E. B. Uncertainties in the central England temperature series since 1878 and some changes to the maximum and minimum series. *Int. J. Climatol*. **25**, 1173–1188 (2005).
61. Moberg, A., Bergström, H., Ruiz Krigsman, J. & Svanered, O. Daily air temperature and pressure series for Stockholm (1756–1998). *Clim. Change* **53**, 171–212 (2002).
62. Hall, J. & Blöschl, G. Spatial patterns and characteristics of flood seasonality in Europe. *Hydrol. Earth Syst. Sci*. **22**, 3883–3901 (2018).
63. Nezhikovskij, R. A. *Reka Neva I Nevskaja Guba*, 81–84 (Leningrad Gidrometeoizdat, 1981).
64. Mudelsee, M., Deutsch, M., Börngen, M. & Tetzlaff, G. Trends in flood risk of the River Werra (Germany) over the past 500 years. *Hydrol. Sci. J*. **51**, 818–833 (2006).
65. Coeur, D. *La plaine de Grenoble face aux inondations* (Versailles Quae, 2008).

Acknowledgements This work was supported by the ERC Advanced Grant 'FloodChange' project (no. 291152), the Horizon 2020 ETN 'System Risk' project (no. 676027), the DFG project FOR 2416, the FWF projects I 3174 and W1219-N22, the Spanish Agency of Science and FEDER/UE projects CGL2016-75475/R, CGL2017-86839-C3-1-R, CGL2016-75996-R and CTM2017-83655-C2-2-R, the ICREA Academia programme, and project CZ.02.1.01/0.0/0.0/16_019/0000797, Ministry of Education, Youth and Sports of the Czech Republic. We acknowledge all flood data providers listed in Extended Data Table 1 and thank J. Lajus for pointing us to the published Neva series.

Author contributions G. Blöschl, A.K. and A.V. designed the study and wrote the first draft of the paper. G. Blöschl initiated the study and provided guidance for the analyses. A.K. collated the database with the help of most of the co-authors and provided guidance for the analyses. A.V. performed all quantitative analyses of the flood data. M. Barriendos, O.B., R.B., D. Coeur, G.D., A.K., M.C.L., N.M., D.R., L.R., P.S.-F., I.A., M. Bělínová, G. Benito, C.B., D. Camuffo, R.D., L.E., S.E., J.C.G., R.G., D. Limanówka, A. P., H.P., F.S.R., C.R., J.S., L.S., L.P.S., W.H.J.T. and O.W. developed historical river flood series. J.H., K.H., M.H., J.K., D. Lun, J.P. and P.V. advised on the data analysis. D. Cornel and J.W. rendered Fig. 1 and the Supplementary Video. All authors interpreted results, and contributed to framing and revising the paper.

Competing interests The authors declare no competing interests.

Additional information

Supplementary information is available for this paper at https://doi.org/10.1038/s41586-020-2478-3.

Correspondence and requests for materials should be addressed to G. Blöschl.

Peer review information *Nature* thanks Anouk Bomers, Francis Ludlow, Olivier Payrastre and the other, anonymous, reviewer(s) for their contribution to the peer review of this work.

Extended Data Fig. 1 | Locations of the flood series. Series indicated by red circles are used for the interpolation of the flood intensities (names as in Extended Data Table 1 and Extended Data Fig. 2). Series indicated by orange circles are supplementary and only used for the seasonality analysis. Thick grey lines indicate regions used in the analysis.

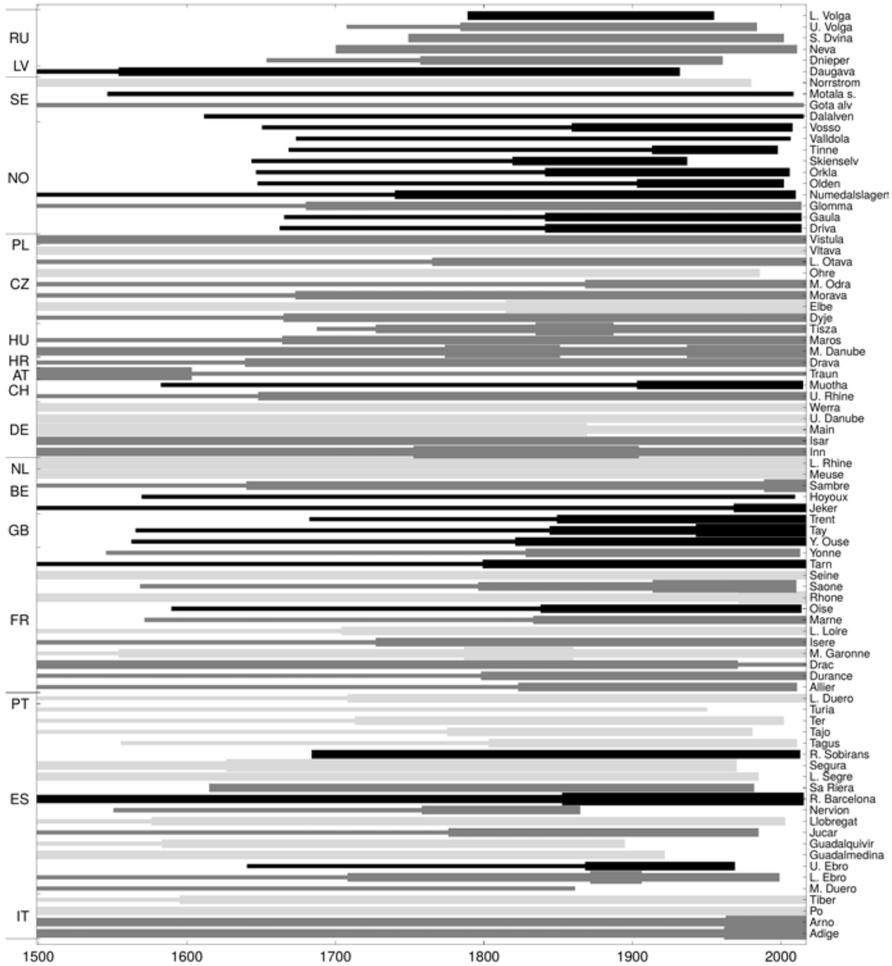

Extended Data Fig. 2 | Duration, representativeness index and bias index of the flood data series. The greyscale refers to the representativeness index that reflects the degree of data representativeness in a regional context (light grey, low representativeness ($u = 1$); dark grey, average representativeness ($u = 2$); black, high representativeness ($u = 3$)). The line width refers to the bias index that reflects the completeness of the source material in a historical context (no line, no data; thin line, period with possibly missing data; average line, average; thick line, period with overly dense data).

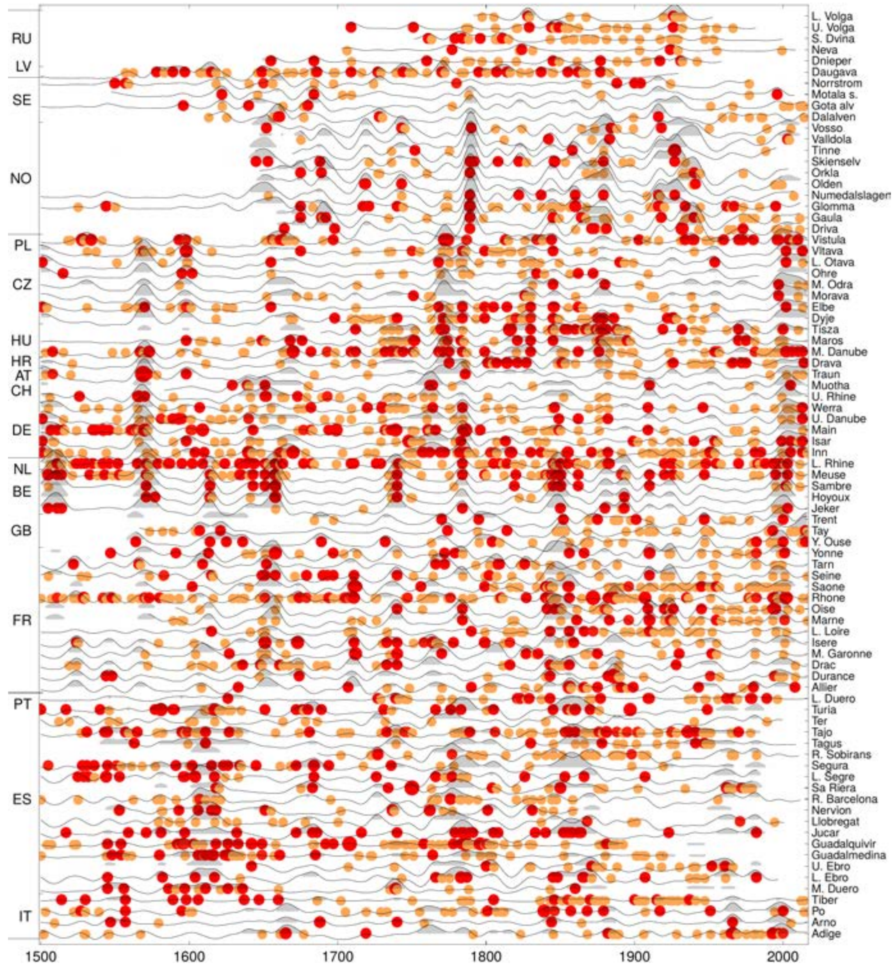

Extended Data Fig. 3 | Raw data of flood intensities. Great (class 2) and extraordinary (class 3) floods are marked by orange and red dots, respectively. Thin lines show the interpolated flood intensities. Flood-rich periods are shown as light grey areas.

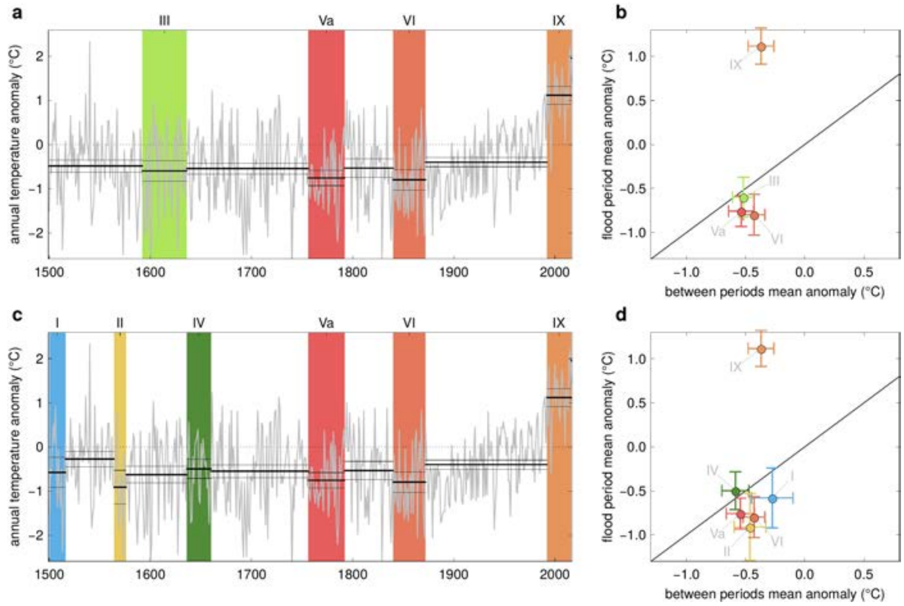

Extended Data Fig. 4 | Anomalies of annual air temperatures. The anomalies are taken from the 1961–1990 mean of annual air temperatures within and outside flood-rich periods in southern Europe (top) and western Europe (bottom). **a**, **c**, Time series of air temperature anomalies (grey line) and their averages and 90% confidence bounds (black lines), and flood-rich periods indicated by colour bars. **b**, **d**, Relationship between mean temperature anomalies in flood-rich periods and those of the intervals in between. Error bars show 90% confidence bounds. Colours correspond to those of the flood-rich periods in **a**, **c**.

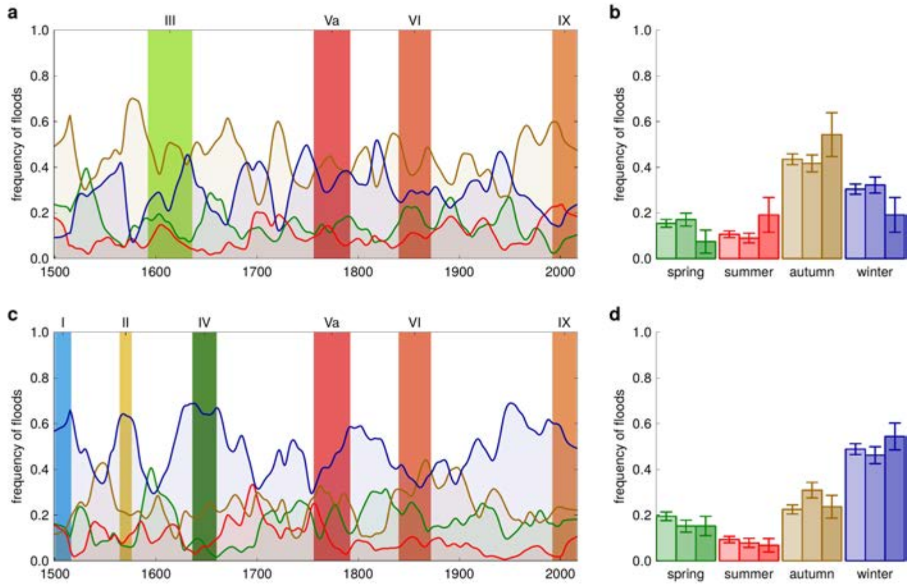

Extended Data Fig. 5 | Flood seasonality. Seasonality of floods is shown within and outside flood-rich periods in southern Europe (top) and western Europe (bottom). **a**, **c**, Time series of smoothed frequency of floods in four seasons (green lines, spring; red, summer; brown, autumn; blue, winter) and flood-rich periods indicated by colour bars. **b**, **d**, Frequency of floods in four seasons. Left bars, interflood periods; middle bars, flood-rich periods of the past; right bars, flood-rich period IX (1990–2016). Error bars show 90% confidence bounds.

Extended Data Table 1 | Flood series, data contributors and countries, involved in the present study

Code of series	Country	Series provider/publication	River flood series	Catchment areas (1000 km²)
RU01, RU03-RU05	Russia (1)	Andrei Panin	Dnieper, Severnaya Dvina, Upper Volga, Lower Volga	504, 357, 236, 1380
RU02	Russia (2)	Published [63]	Neva	281
LV01	Latvia	Andrei Panin	Daugava	88
SE01-SE04	Sweden	Dag Retsö	Dalalven, Gota alv, Motala strom, Norrstrom	29, 50, 15, 23
NO01-NO10	Norway	Lars Roald	Driva, Gaula, Glomma, Numedalslagen, Olden, Orkla, Skienselv, Tinne, Valldola, Vosso	2.5, 3.7, 41, 56, 0.6, 3.1, 11, 0.2, 1.1, 1.5
PL01-PL02	Poland	Radosław Doktor, Danuta Limanówka	*Upper Odra*, Vistula	106, 51
CZ01-CZ05, CZ08	Czech Republic (1)	Rudolf Brázdil	Dyje, Elbe, Morava, Middle Odra, Ohře, Vltava	11, 51, 21, 7.2, 113, 4.6, 28
CZ06-CZ07	Czech Republic (2)	Líbor Elleder	Lower Otava, *Upper Otava*	2.9, 0.5
HU01-HU03	Hungary	Andrea Kiss	Middle Danube, Maros, Tisza	210, 27, 157
HR01	Croatia	Hrvoje Petrić	Drava	40
AT01-AT02	Austria	Christian Rohr, Andrea Kiss	Traun, *Wien*	4.1, 0.2
CH02, CH04, CH06-CH11	Switzerland (1)	Petra Schmocker-Fackel	*Alpenrhein, Emme,* Muotha, *Schächen, Sihl, Sitter, Thur, Umäsch*	6.2, 0.4, 0.3, 0.1, 0.3, 0.3, 1.7, 0.07
CH01	Switzerland (2)	Oliver Wetter	Upper Rhine	30
CH03, CH05	Switzerland (3)	Lothar Schulte	Aare, *Lutschine*	0.03, 0.4
DE05-DE06	Germany (1)	Rüdiger Glaser, Johannes Schönbeim	Main, Upper Danube	27, 7.5
DE01-DE04, DE07	Germany (2)	Oliver Böhm	Inn, *Iller*, Isar, Lech, *Salzach*	12, 1.0, 4.1, 3.9, 6.6
DE08	Germany (3)	Published [64]	Werra	5.5
NL01	Netherlands	Willem H.J. Toonen	Lower Rhine	185
BE01-BE04	Belgium	Gaston Demaree	Jeker, *Hoyoux*, Sambre, Meuse	0.5, 0.3, 2.7, 36
GB01-GB03	United Kingdom	Neil Macdonald	Yorkshire Ouse, Tay, Trent	3.3, 4.6, 7.5
FR01-FR02, FR04-FR05, FR07-FR015	France (1)	Denis Coeur	Allier, Durance, Middle Garonne, Upper Garonne, *Middle Loire*, Lower Loire, Marne, Oise, Rhône, Saone, Seine, Tarn, Yonne	14, 14, 52, 14, 39, 117, 13, 17, 96, 30, 44, 9.7, 11
FR03, FR06	France (2)	Published [65]	Drac, Isere	3.6, 9.5
PT01	Portugal	Inês Amorim, João Carlos Garcia, Luís Pedro Silva	Lower Duero	98
ES01-ES16, ES18-ES20	Spain (1)	Mariano Barriendos	Middle Duero, Lower Ebro, Upper Ebro, Guadalmedina, Guadalquivir, Jucar, Llobregat, Nervion, *Pisuerga*, Rieres Pla de Barcelona, Sa Riera Mallorca, *Upper Segre*, *Middle Segre*, Lower Segre, Segura, R. Sobirans, Tajo, Ter, Turia	40, 79, 15, 0.2, 57, 22, 4.9, 1.9, 15, 0.1, 0.1, 1.2, 1.7, 20, 20, 0.03, 82, 1.8, 6.4
ES17	Spain (2)	Gerardo Benito	Tagus	9.3
IT01-IT04	Italy	Silvia Enzi, Dario Camuffo, Chiara Bertolin	Adige, Arno, Po, Tiber	12, 8.2, 74, 17

Italics indicate that the series was only used for the seasonality analysis (denoted 'Supplementary' in Extended Data Fig. 1). The code of the series (first column) consists of the country code and a running number. Some data[63–65] are published elsewhere.

Extended Data Table 2 | Flood-rich periods in Europe in the past 500 years

Period	Full time period	Core time period	Core duration (yrs)	Regions	Max area ($10^6 km^2$)	Volume ($10^6 km^2$ yrs)	Scaled volume	Scaled mean intensity	Rank
I	1500-1520	1500-1516	17	Western Europe, Central Europe	0.569	5.97	0.282	0.622	9
II	1560-1580	1564-1576	13	Western Europe, Central Europe	0.923	8.76	0.416	0.826	4
III	1590-1640	1592-1636	45	Iberia, Southern France	1.025	18.08	0.864	0.269	6
IV	1630-1660	1636-1660	25	Western Europe, West-Central Europe, Northern Italy	0.891	9.71	0.462	0.602	7
Va	1750-1800	1756-1792	37	Central Europe, Western Europe	1.830	20.92	1.000	0.627	1
Vb	1750-1800	1788-1792	5	Scandinavia	0.496	3.75	0.176	1.000	5
VI	1840-1880	1840-1872	33	Western Europe, Southern Europe	1.621	19.86	0.949	0.637	2
VII	1860-1900	1864-1892	29	East Central Europe	0.411	5.62	0.266	0.657	8
VIII	1910-1940	1916-1940	25	Scandinavia	0.573	5.71	0.270	0.627	10
IX	1990-2016	1992-2016	25	Western Europe, Central Europe, Italy	1.771	18.69	0.893	0.607	3

Full time periods obtained by generalizing the core time periods, core time periods resulting from the analysis, durations of the core periods, regions, maximum area, volume (that is, space–time domain covered by period), scaled volume, scaled mean intensity of the interpolated flood intensity, and rank. Scaling is from 0 to 1 for the 74 periods identified.

from a C–G base pair to T–A, occurred about 5–50% of the time. The efficiency of editing was influenced by various factors: the spacing between the two DdCBE subunits; TALE design; orientation of the split-DddA$_{tox}$ halves; and the position of the target cytosine relative to the TALE bindings sites.

A major consideration for all genome-editing tools is whether they modify DNA at unintended sites. Mok and colleagues compared treated and untreated cells, and found no off-target effects in the nuclear genome. Off-target activity in mtDNA was low, except in the case of one gene, in which off-target edits were linked to the TALE design.

Next, Mok *et al.* examined the therapeutic potential of DdCBE. The authors reported that cytosine base editing has the potential to correct 49% of known harmful mtDNA mutations. However, in its current form, DdCBE can efficiently edit only C bases that are preceded in the genome by a T, narrowing its range.

The reliance of DdCBE on DNA replication to implement the C–G to T–A conversion implies a theoretical maximum editing efficiency of 50%. To explain, the two newly replicated mtDNAs each receive a parental DNA strand, one of which will be unedited, containing G, which becomes paired with a C. However, Mok *et al.* find that the activity of DdCBE persists over several days, potentially offering the opportunity for further editing during subsequent replication events. Whether off-target effects increase during prolonged exposure to DdCBE will be a key consideration for the future.

These caveats mean that DdCBE might cause a reduction in — rather than complete elimination of — mtDNA mutations. But given that the severity of the symptoms of mtDNA diseases increases with mutation load[8], the ability to reduce the mutation level in itself holds therapeutic promise.

Mitochondrion-targeted nucleases have previously been used to eliminate specific mtDNA mutations in mice[9,10]. This is possible because the double-strand breaks they create lead to mtDNA degradation. Cells contain many copies of their mtDNA, and only the copies that carry the harmful mutation are degraded. But there is a risk that, in cases of high mutation load, elimination of mutated mtDNA could reduce the mtDNA copy number to harmfully low levels. And the nuclease approach could not be used if all copies of mtDNA carry the same mutation. By contrast, base editing could reduce the fraction of mtDNA that carries a mutation without reducing the copy number. It might therefore be the preferred (or the only) option when the mutation load is high.

Does DdCBE have the potential to prevent the transmission of mtDNA disease? MtDNA is typically inherited only from mothers, and current mitochondrial-replacement procedures reduce the transmission of mtDNA mutations by transplanting the nuclear genome from the egg of a woman who carries the mutated mtDNA into an unaffected donor egg[11]. Base editing to reduce the mutation load in eggs or early embryos could theoretically be an alternative approach. However, mtDNA replication is thought not to occur during the first five to six days of human development[12], and so success might hinge on prolonged protection of U.

Mok and colleagues' work is a key advance towards the development of gene therapies for mtDNA diseases. In addition, by using the tool to experimentally alter the mitochondrial genome, we could gain a better understanding of the relevance of mtDNA mutations in complex diseases, cancer and age-related cellular dysfunction. The study is also likely to inspire further developments in protein engineering and evolution that increase the range and efficiency of DdCBE, and to intensify the search for other promising candidate base editors.

Magomet Aushev and **Mary Herbert** are in the Wellcome Centre for Mitochondrial Research, Biosciences Institute, Centre for Life, Newcastle upon Tyne NE1 4EP, UK.
e-mails: mag.aushev@newcastle.ac.uk; mary.herbert@newcastle.ac.uk

1. Russell, O. M., Gorman, G. S., Lightowlers, R. N. & Turnbull, D. M. *Cell* **181**, 168–188 (2020).
2. Mok, B. Y. *et al. Nature* **583**, 631–637 (2020).
3. Salter, J. D. & Smith, H. C. *Trends Biochem. Sci.* **43**, 606–622 (2018).
4. Moretton, A. *et al. PLoS ONE* **12**, e0176795 (2017).
5. Schmidt, O., Pfanner, N. & Meisinger, C. *Nature Rev. Mol. Cell Biol.* **11**, 655–667 (2010).
6. Gammage, P. A., Moraes, C. T. & Minczuk, M. *Trends Genet.* **34**, 101–110 (2018).
7. Kunz, C., Saito, Y. & Schär, P. *Cell. Mol. Life Sci.* **66**, 1021–1038 (2009).
8. Hellebrekers, D. M. E. I. *et al. Hum. Reprod. Update* **18**, 341–349 (2012).
9. Bacman, S. R. *et al. Nature Med.* **24**, 1696–1700 (2018).
10. Gammage, P. A. *et al. Nature Med.* **24**, 1691–1695 (2018).
11. Greenfield, A. *et al. Nature Biotechnol.* **35**, 1059–1068 (2017).
12. St. John, J. C., Facucho-Oliveira, J., Jiang, Y., Kelly, R. & Salah, R. *Hum. Reprod. Update* **16**, 488–509 (2010).

This article was published online on 8 July 2020.

Historical climatology

A flood history of Europe

Francis Ludlow & Rhonda McGovern

Europe's rich heritage of historical documents has been used to reconstruct the flooding history of the continent for the past five centuries. This could help policymakers to develop flood-management strategies for the future. **See p.560**

On page 560, Blöschl *et al.*[1] capitalize on a vast assembly of written historical observations to provide a history of flooding for 103 major European river reaches between AD 1500 and 2016. In doing so, they reveal nine flood-rich periods that affected extensive regions in distinct areas of Europe — and find that the most recent of these periods, which might not yet be over, differs in key respects from the others.

Some 0.03% of the European population, on average, are thought to have been affected by flooding annually between 1870 and 2016, at a yearly average cost of 0.8–0.9% of gross domestic product[2]. Increased flood hazards are widely expected in the future for a substantial area of Europe as a result of climate change[2], and so, without effective management and adaptation, these losses will potentially be even greater.

Such measures must be based on the best available knowledge, and require an understanding of long-term flooding patterns. Decision makers must know whether they are living in a flood-rich period (more-frequent flooding, of higher magnitudes or greater extent than usual) or a flood-poor one (fewer floods, with lower magnitudes or less-than-usual extent). Extreme floods in any one river basin in a given year are inherently rare, but the risk is cumulatively higher across large regions such as Europe — so the longer and more spatially extensive these flood histories are, the better.

Fortunately, Europe hosts some of the most abundant and diverse historical documentary sources for any world region, ranging from annals and chronicles to administrative and legal records, correspondence and newspapers (Fig. 1). These sources are replete with observations of extreme weather and hazards such as flooding, given their often severe human impacts, spectacular effects and religious significance as portents or vehicles of divine retribution[3]. For example, the Gaelic Irish *Annals of Connacht* for AD 1471 reports[4]: "Showers of hail fell [on] each side of Beltaine [1st May], with lightning and thunder, destroying much blossom and beans and fruits in all parts of Ireland where they fell. One of these showers, in the east, had stones two or three inches long, which made large wounds on the people they struck ... There was another ... at the monastery of Boyle; and a boat could have floated over the floor of the great church of the monks, as we have heard from the folk of that place."

This account highlights the strengths of documentary evidence: it is precisely dated, highly spatially resolved, generally unambiguous about the meteorological conditions involved and explicit regarding human impacts. Such evidence is used as the basis of historical climatology, a field whose origins date back to at least the 1920s (ref. 5), and which accelerated in the 1960s and 1970s, thanks to pioneers such as Hubert Lamb and Hermann Flohn. Their work furthered the growing recognition that societally meaningful changes in climate had occurred throughout the past few centuries, eroding the idea that the long-term climate was more or less constant during that period[6].

Yet despite continued development of the field, historical climatologist Christian Pfister and climate scientist Heinz Wanner remarked[7] in 2002 that "many scientists are of the opinion that observations made before the instrumental period are "subjective" and less reliable than natural proxies ...". They went on to argue that "once calibrated and verified ... the data are precise and have a spatiotemporal resolution unmatched by any other climate proxy". Since then, historical climatologists have continued to identify evidence, develop methods to assess its credibility and quantify it to reconstruct past climates[8–10]. With their compilation of 9,576 floods, Blöschl *et al.* have built on this foundation to deliver a major contribution to our understanding of European flood history.

Patterns of past precipitation are inherently more spatially variable, and hence harder to reconstruct, than are those of temperature. Reconstructing flooding is even more challenging, because flooding depends not only on precipitation, but also on human landscape usage, from upstream deforestation to damming, bridging and urbanization. It is also related to prevailing temperatures, which have a seasonally and regionally varying role across Europe, influencing evaporation and soil moisture and the timing of spring snowmelt[11]. Importantly, therefore, Blöschl and colleagues establish an association in timing between all but one flood-rich period and the prevalence of lower-than-usual average temperatures. By contrast, the most recent flood-rich period in Europe (1990 to 2016, when the available data end) — for a region stretching into western and central Europe and northern Italy, and defined by the authors as being one of the most severe — is exceptional for occurring in a warming climate.

Just one highlight of this work is the care taken to control for biases arising from variability in the type and abundance of sources

EDGAR SU/REUTERS

Figure 1 | Historical evidence of flooding. This reproduction of a woodcut depicts inundation of the streets of Glauchau in Germany in 1854. Blöschl *et al.*[1] have used information from historical records to construct a flood history for Europe from 1500 to 2016.

through space and time, a persistent challenge often acknowledged but infrequently addressed[3]. A further standout feature is the authors' 3D visualization of the magnitude, duration and geography of each flood-rich period (see Fig. 1 of the paper[1] and Supplementary Video 1). This invites a consideration of the internal and external climate processes that potentially drove these periods, and how their regional expression was manifested in, or mediated by, the behaviour of major modes of ocean and atmospheric circulation.

One key suspect noted by Blöschl *et al.* is the North Atlantic Oscillation (NAO), a fluctuation in the atmospheric pressure gradient between Iceland and the Azores that governs the strength and positioning of moisture-laden winter westerlies (and accompanying storm tracks) over Europe. Depending on the strength of this gradient, the westerlies either bring relatively warm wind and rain to northern and northwestern Europe, leaving southern Europe dry and cool, or flow towards southern Europe, leaving northern and northwestern Europe to experience incursions of cold and dry Arctic air.

But ambiguities remain regarding the mechanisms at play. With the dominant flood season differing by region (winter for northern and northwestern Europe, but summer for central Europe, for example), the wintertime NAO can explain only part of this story. The related role of prevailing temperatures in the observed flood-rich periods also remains an open question. Earth-system modelling, twinned with process-based hydrological models (as the authors note) could be used to capture the complexity of natural and human processes on the ground that enhance or suppress flooding. It could also provide further insight into the extent to which the association of cooler-than-usual conditions with most flood-rich periods is causative or correlative, and how much the most recent flood-rich period is a result of human-induced climate warming.

Blöschl *et al.* clearly demonstrate the potential of historical climatology, but there are yet more avenues by which to advance this approach to reconstruct past climate. Written evidence of climate can become particularly discontinuous in the deep past, but tree-ring evidence, for example (measurements of tree-ring widths, densities and isotopic composition, which correlate with climate conditions), is more continuous over long periods. However, tree-ring evidence usually reflects only the growing-season climate, whereas written evidence can attest to weather for all seasons. If both sources were more regularly used in a complementary manner[12], it would improve our understanding of the climatic signals preserved in each source, and help to resolve perceived conflicts — for instance, the great European drought of AD 1540 is readily apparent in written records, but more ambiguously represented in certain tree-ring evidence[13].

Further written sources remain to be discovered, including documents known as weather diaries, which are highly prized in historical climatology for their standardized systematic recording of weather conditions. These can be found not only in the most recent centuries, but sometimes much earlier — as with the incredible Babylonian 'astronomical diaries'[14], which boast systematic daily observations of weather during the first seven centuries BC, and which remain largely unexploited. As Pfister and Wanner stated[7] in 2002, "Worldwide, many thousand volumes with daily observations exist, but have not yet been analyzed for their climatic information. Let's get to work!"

Francis Ludlow and **Rhonda McGovern** are at the Trinity Centre for Environmental Humanities, School of Histories and Humanities, Trinity College, Dublin D02 PN40, Ireland.
e-mail: ludlowf@tcd.ie

1. Blöschl, G. *et al. Nature* **583**, 560–566 (2020).
2. Paprotny, D., Sebastian, A., Morales-Nápoles, O. & Jonkman, S. N. *Nature Commun.* **9**, 1985 (2018).
3. Ludlow, F. in *At the Anvil: Essays in Honour of William J. Smyth* (eds Duffy, P. J. & Nolan, W.) Ch. 5 (Geography Publs, 2012).
4. Freeman, A. M. (ed.) *Annála Connacht: The Annals of Connacht, A.D. 1224–1544* (Dublin Inst. Advanced Studies, 1944).
5. Brooks, C. E. P. *Q. J. R. Meteorol. Soc.* **54**, 309–317 (1928).
6. Chambers, F. M. & Brain, S. A. *Holocene* **12**, 239–249 (2002).
7. Pfister, C. & Wanner, H. *Past Glob. Changes Mag.* **10**, 2 (2002).
8. Brázdil, R., Pfister, C., Wanner, H., Von Storch, H. & Luterbacher, J. *Clim. Change* **70**, 363–430 (2005).
9. White, S., Pfister, C. & Mauelshagen, F. (eds) *The Palgrave Handbook of Climate History* (Palgrave Macmillan, 2018).
10. Camenisch, C., Bauch, M., Huhtamaa, H., Pei, Q. & White, S. *Past Glob. Changes Mag.* **27**, 73 (2019).
11. Blöschl, G. *et al. Nature* **573**, 108–111 (2019).
12. Gao, C., Ludlow, F., Amir, O. & Kostick, C. *Quat. Int.* **394**, 180–193 (2016).
13. Pfister, C. *et al. Clim. Change* **131**, 191–198 (2015).
14. Huijs, J., Pirngruber, R. & van Leeuwen, B. in *A History of Market Performance: From Ancient Babylonia to the Modern World* (eds van der Spek, R. J., van Leeuwen, B. & van Zanden, J. L.) 128–148 (Routledge, 2015).

Human migration

Native South Americans reached Polynesia early

Paul Wallin

DNA analysis of Polynesians and Native South Americans has revealed an ancient genetic signature that resolves a long-running debate over Polynesian origins and early contacts between the two populations. **See p.572**

For many years, scholars have speculated about how Polynesia was initially populated. On page 572, Ioannidis *et al.*[1] now describe a genetic approach that they used to address the issue of Polynesian origins and interactions.

The early peopling of Polynesia attracted worldwide interest in 1947, when the Norwegian explorer Thor Heyerdahl set sail on the *Kon-Tiki* expedition to test his migration theory[2]. The crew left Peru on a wooden raft, and after 101 days and a voyage of more than 7,000 kilometres, they reached Polynesian shores, thus demonstrating the possibility of early travel from South America to these Pacific islands. Heyerdahl challenged the scientific community's view that evidence pointed instead to the peopling of Polynesia by people travelling east from Asia, and his idea that Polynesia was initially populated by South Americans was generally criticized by scholars.

The same scientific community nevertheless discussed cultural contacts between the two regions, because a South American plant, the sweet potato, has a long history of cultivation in eastern Polynesia. The idea that Polynesians voyaged to South America and introduced the plant on their return to Polynesia became the accepted explanation for this[3]. Rapa Nui (also known as Easter Island) is the best-known example considered concerning such contacts[4]. It is a part of Polynesia that is located relatively close to South America, and in Rapa Nui there is evidence of large, ancient sweet-potato fields, extraordinary old stonework and a specific birdman cult – all of which are features in common with those of South America.

Ioannidis and colleagues analysed the DNA of people from Rapa Nui, and also studied DNA of individuals from 17 populations of Pacific islands and 15 Native American populations from the Pacific coast of South America. Genome-wide DNA analyses of 807 people (analysing predominantly present-day individuals) enabled the authors to search for evidence of ancestors from different populations who produced offspring together – thereby generating a combined genetic signature of the two populations, described as an admixture. The authors compared the dominant Polynesian DNA markers with those of people from other regions, including Europe, America, Africa and Melanesia. A computational method called an ADMIXTURE analysis allowed Ioannidis and colleagues to work out a person's probable genetic ancestry and ancestral geographical origins through studies of gene flow. Their main discovery is that several eastern Polynesian populations have signs of a background signature (genetic traces from distant ancestors) that originated from Native South American people.

> **"Future research should assess the possibility of more than just one early contact from South America."**

How did Ioannidis and colleagues solve this complex task of genetic unravelling? In their admixture studies, they could trace and distinguish between different modern colonial admixtures; for example, in French Polynesia, there was a large French influence, whereas Spanish and Chilean groups were part of the population history in Rapa Nui. A key discovery came from their analysis of people from Rapa Nui – a signature could be assigned to Native South American populations from northern coastal regions of South America, and this component was independent of other large historical, or more-recent, admixture events. This signature exists in the genetic background, indicating that it is an old and stable hallmark of admixture. A surprising finding is that this signal was also identified in other eastern Polynesian populations, for example in populations in Mangareva, in North Marquesas and South Marquesas, and in Palliser in the Tuamotu Islands (Fig. 1). These other islands lie farther from South America than does Rapa Nui, although for people sailing from South America they are destinations that would be aided by favourable trade winds and currents.

Ioannidis *et al.* investigated the estimated timing of admixture events using a method called tract-length distribution analysis, which assesses the length distributions of the genomic segments inherited from different ancestral populations. As expected, this statistical approach suggests that the European admixtures in Polynesia first date back to colonial phases of AD 1750–1860.

The authors made the notable discovery that an initial admixture event between Native South Americans and Polynesians took place in eastern islands of Polynesia around AD 1150–1230. Previous work[3,5] is consistent with a model of populations spreading eastwards from Asia possibly having reached eastern Polynesia by that time. The exception to this South American admixture timeframe is Rapa Nui, which had a later admixture, dated to around AD 1380. This later date for Rapa Nui is surprising, because it is the closest site to South America studied and has been cited as the 'typical' example of a location with possible early connections to South America. However, the timing difference might be due to a more complex genetic history there because of relatively recent Chilean genetic input.